Polyhedron xxx (2016) xxx–xxx

Contents lists available at ScienceDirect

Polyhedron

journal homepage: www.elsevier.com/locate/poly

Ruthenium complexes of phosphino derivatives of carboxylic amides: Synthesis and characterization of tridentate P,E_2 and tetradentate P,E_3 (E = N,O) ligands and their reactivity towards [$RuCl_2(PPh_3)_3$]

Robert Gericke, Jörg Wagler *

Institut Für Anorganische Chemie, Technische Universität Bergakademie Freiberg, D-09596 Freiberg, Germany

ARTICLE INFO

Article history:
Received 5 July 2016
Accepted 22 August 2016
Available online xxxx

Keywords:
Ambidentate ligands
Chelates
NMR spectroscopy
Ruthenium
Single-crystal X-ray diffraction

ABSTRACT

Neutral bi- and tripodal ligands of the type $Ph_xP(\mathbf{L})_{3-x}$ (x = 1 (for **1**), 0 (for **2**); **L** = *N*-methylbenzamidyl (**La**, **1a**, **2a**), phthalimidyl (**Lb**, **1b**, **2b**), 2-pyridyloxy (**Lc**, **1c**, **2c**)) have been synthesized to act as P,O (**1a**, **1b**, **2a**, **2b**) or P,N (**1c**, **2c**) chelating ligands in the ruthenium coordination sphere. Reactions of the ruthenium source [$RuCl_2(PPh_3)_3$] with **1a**,**b**,**c** and **2b**,**c** result in the formation of *all-cis* bis-chelate complexes [$RuCl_2(PPh_3)\kappa$-P,O,O- or κ-P,N,N-($Ph_xP(\mathbf{L})_{3-x}$)] **3a**,**b**,**c** (x = 1) and **4b**,**c** (x = 0), respectively. Surprisingly, during the reaction of [$RuCl_2(PPh_3)_3$] with **2a** a P–N bond cleavage in favor of P=O bond formation takes place with formation of complex **5a** [$RuCl(PPh_3)_2\kappa$-P,O,O-(O=P(**La**)$_2$)]. Treatment of the reaction mixture with $TlPF_6$ afforded the phosphonium salt **6** [$Ph_3P(Ph)C{=}NMe]PF_6$. Attempts to form similar compounds to **5a** with **Lb** or **Lc** (driven by chloride abstraction upon addition of $TlPF_6$) only afforded the cationic complexes of the type [$RuCl(PPh_3)_2\kappa$-P,O,O- or κ-P,N,N-(P(**L**)$_3$)]PF_6 (**L** = **Lb** (**7b**), **Lc** (**7c**)). All isolated compounds were characterized with multi-nuclear NMR spectroscopy, single-crystal X-ray diffraction (except **4c**) and elemental analysis.

1. Introduction

Recently we reported the syntheses of diphenylphosphino functionalized derivatives **Ph_2P-L** of *N*-methylbenzamide (**HLa**), phthalimidine (**HLb**) and pyridine-2-one (**HLc**) and we have shown their P,O- (for **L** = **La**, **Lb**) or P,N-bidentate (for **L** = **Lc**) ligand behavior towards ruthenium [1]. In analogy to these diphenylphosphino functionalized carboxy amides, we synthesized the monophenylphosphino derivatives and the phosphino derivatives (with $PhPCl_2$ or PCl_3 and a base, *n*-BuLi for reactions with **HLa** and triethylamine for reactions with **HLb** and **HLc**). Similar series of P,O-ambidentate phosphine functionalized amides $Ph_xP(\mathbf{L})_{3-x}$ (x = 2,1,0; **L** = 1,8-naphtholactamyl [2] (**A**), **L** = 3,3,4,4-tetramethylsuccinimidyl [3] (**B**)) and of P,N-ambidentate ligands, such as $Ph_xP(\mathbf{L})_{3-x}$ with x = 2,1,0; **L** = *ortho*-*N*-methylanilinyl [4] (**C**) or **L** = 2-picolyl [5–7] (**D**) are mentioned in the literature (Scheme 1). Those and related bi-, tri- and tetradentate ligands show a high flexibility in there coordination behavior towards transition metals [2,7–9] (**E**–**H**). Whereas in **H** the basically tripodal PN_3 ligand acts as a tridentate chelator at ruthenium, tripodal PP'_3 ligands were shown to form Ru-tripod complexes with hexacoordinated Ru atom (**I**,**J**,**K**,**L**) [10–13]. For some other transition metals (TM) it has been shown that tripodal ligands of the type PE_3 with E = 2nd row elements can form tripod complexes TM(κ^4-PE_3) as well (**M**,**N**,**O**) [14–16]. As pointed out in our recent report [1], P,O ligands of the type *N*-phosphino functionalized carboxylic amide, we found a lack of literature reports for the coordination behavior towards the catalytically highly active transition metal ruthenium, which serves as a motivation for us to investigate this coordination chemistry for four related P,O ligands (bipodal **1a**, **1b**; tripodal **2a**, **2b**, Scheme 2) and, for comparison, for two barely explored P,N ligands (bipodal **1c**, tripodal **2c**) [8,17], which can be interpreted as *O*-phosphino functionalized carboxylic amides.

2. Experimental

2.1. General considerations

All preparations were carried out under an atmosphere of dry argon using standard Schlenk techniques. Phthalimidine [18] and *N*-methylbenzamide [19] were prepared following literature methods. Tetrahydrofuran (THF) and triethylamine were distilled from sodium/benzophenone and stored under dry argon. Dichloromethane (DCM) was distilled from calcium hydride and stored under argon. Chloroform (stabilized with amylenes) was stored

* Corresponding author. Fax: +49 3731 39 4058.
E-mail address: joerg.wagler@chemie.tu-freiberg.de (J. Wagler).

http://dx.doi.org/10.1016/j.poly.2016.08.041
0277-5387/

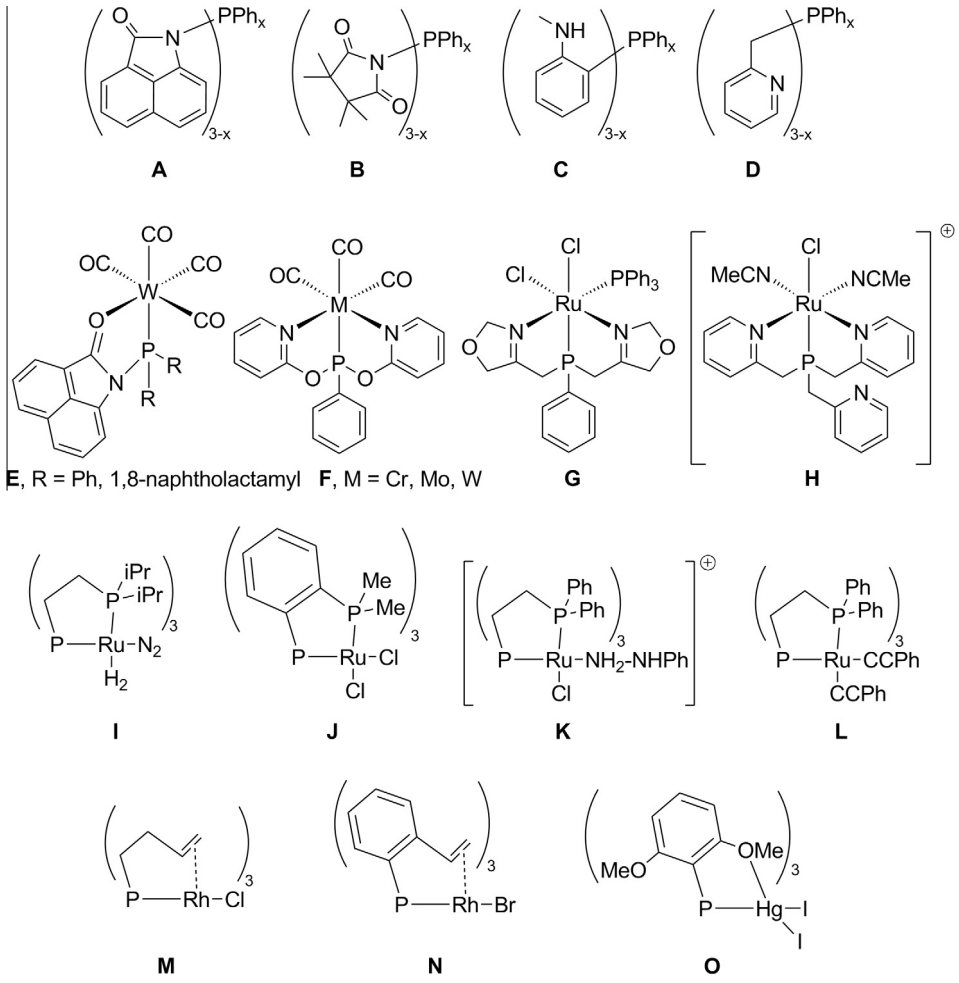

Scheme 1. Examples of neutral P,N and P,O ligands of the series $Ph_xP(L)_{3-x}$ (x = 0, 1, 2) (A–D), examples of transition metal complexes using di-, tri- or tetradentate neutral P,N and P,O chelating ligands (E–H), examples of tripodal RuP_4 complexes (I–L) and examples of tripodal transition metal complexes with tripod arms out of 2nd row elements (M–O).

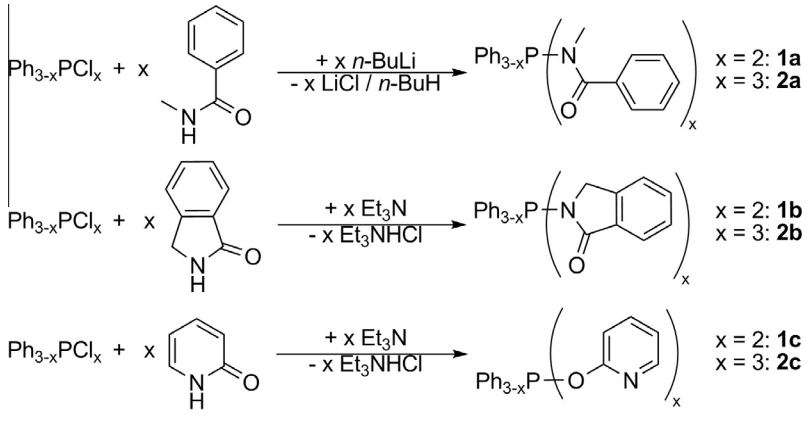

Scheme 2. Synthesis of compounds **1a**, **1b**, **1c**, **2a**, **2b** and **2c**.

over molecular sieves 3 Å. $[RuCl_2(PPh_3)_3]$ was synthesized as reported earlier [1]. All other chemicals used were commercially available and were used without further purification. Elemental microanalyses (C, H, N) were performed on a 'Vario Micro Cube' analyzer (Elementar, Hanau, Germany).

2.2. NMR spectroscopy

NMR spectra of solutions were recorded on an 'Avance 500' or 'Ascend 400' spectrometer (Bruker Biospin, Rheinstetten, Germany) and internally referenced to tetramethylsilane for ^1H

and ^{13}C and externally referenced to 85% H_3PO_4 for ^{31}P. Signals were assigned by using $^{1}H,^{1}H$-COSY, $^{1}H,^{13}C$-HSQC, $^{1}H,^{13}C$-HMBC and $^{1}H,^{1}H$-NOESY spectroscopy. Individual schemes for signal assignment are provided with each complex (where applicable).

2.3. X-ray crystallography

Single-crystal X-ray diffraction data sets were collected with ω-scans on an 'IPDS-2(T)' diffractometer (STOE, Darmstadt, Germany) using Mo Kα-radiation. The absorption correction was performed with XSHAPE using integration correction type. Structures were solved by direct methods with SHELXS [20] and all non-hydrogen atoms were anisotropically refined in full-matrix least-squares cycles against $|F^2|$ (SHELXS) [21]. Hydrogen atoms were placed in idealized positions and refined isotropically (riding model). Selected parameters of data collection and refinement of the herein presented structures are listed in the Supporting information.

2.4. Syntheses of ligands **1a**, **1b**, **1c**, **2a**, **2b** and **2c**

1a: *N*-Methylbenzamide (1.01 g, 7.50 mmol) was dissolved in THF (20 mL) and cooled with an ice/ethanol mixture (to ca. −10 °C). A solution of 2.5 M *n*-BuLi in hexanes (3 mL, 7.50 mmol) was added dropwise. The white suspension was stirred with cooling for 1.5 h and subsequently allowed to attain room temperature. Dichlorophenylphosphine (671 mg, 3.75 mmol) was added with stirring and the pale yellow suspension was stirred for 3 h at ambient temperature. Thereafter, the volatiles of the mixture were evaporated (condensed into a cold trap under reduced pressure) and the solid residue was dispersed in hot $CHCl_3$ (20 mL) for 30 min. After cooling to room temperature the suspension was filtered through Celite. From the filtrate the solvent was removed *in vacuo* and the residue was recrystallized in THF (1.8 mL). The white crystalline product was suitable for single-crystal X-ray diffraction. The supernatant was removed by decantation, the white solid was washed with 3 mL Et_2O and dried *in vacuo* to yield 0.678 g (1.69 mmol, 45%) of **1a**. Although the crystal structure reveals the formation of a THF solvate **1a**·0.75THF, the composition upon drying corresponds to the solvent free compound diluted by some inert (non-C/H/N) material, which most likely is the byproduct LiCl.

Anal. Calc. for $C_{22}H_{21}N_2O_2P$·0.6LiCl (MW: 401.82), requires: C, 65.76; H, 5.27; N, 6.97. Found: C, 65.78; H, 5.28; N, 6.82%. ^{1}H NMR ($CDCl_3$, δ ppm): 3.12 (d, J = 0.67 Hz, -CH_3, 6H), 7.16 (m, aryl, 4H), 7.23 (m, aryl, 4H), 7.27 (m, aryl, 2H), 7.41 (m, aryl, 2H), 7.49 (m, aryl, 1H), 7,55 (m, aryl, 2H). $^{13}C\{^{1}H\}$ NMR ($CDCl_3$, δ ppm): 33.7 (d, J = 6.5 Hz), 127.8 (d, J = 7.15 Hz), 127.9 (s), 129.6 (s), 129.7 (d, J = 22.5 Hz), 130.0 (d, J = 2.0 Hz), 130.2 (s), 133.7 (d, J = 14.0 Hz), 135.8 (d, J = 3.2 Hz), 176.7 (d, J = 35.9 Hz). $^{31}P\{^{1}H\}$ NMR ($CDCl_3$, δ ppm): 85.4 (s).

1b: Phthalimidine (800 mg, 6.01 mmol) was dissolved in THF (40 mL). At ambient temperature triethylamine (670 mg, 6.62 mmol) was added dropwise and the mixture was stirred for 5 min, whereupon dichlorophenylphosphine (538 mg, 3.01 mmol) was added and the mixture was stirred for one day. Thereafter the white precipitate was filtered and washed with THF (3 mL). The combined filtrate and washings were evaporated to dryness (condensation of volatiles into a cold trap under reduced pressure), the residue was dissolved in THF (10 mL) and the solution was filtered through Celite. After vapor diffusion of *n*-pentane into the filtrate (for one week), white crystalline product suitable for single-crystal X-ray diffraction was obtained. The supernatant was removed by decantation, the white solid was washed with *n*-pentane (3 mL) and dried *in vacuo* to yield 480 mg (1.29 mmol, 43%) of **1b**.

Anal. Calc. for $C_{22}H_{17}N_2O_2P$ (MW: 372.36), requires: C, 70.96; H, 4.60; N, 7.52. Found: C, 70.77; H, 4.67; N, 7.50%. ^{1}H NMR ($CDCl_3$, δ ppm): 4.72 (d, J = 17.11 Hz, –CH_2–, 2H), 4.87 (d, J = 17.11 Hz, –CH_2–, 2H), 7.39–7.50 (m, aryl, 7H), 7.53–7.62 (m, aryl, 4H), 7.84 (d, J = 7.59 Hz, aryl, 2H). $^{13}C\{^{1}H\}$ NMR ($CDCl_3$, δ ppm): 52.90 (d, J = 11.9 Hz), 123.6 (s), 124.8 (s), 128.5 (s), 129.3 (d, J = 5.7 Hz), 130.3 (s), 131.1 (d, J = 22.4 Hz), 132.0 (s), 133.1 (s), 134.1 (s), 144.8 (d, J = 6.0 Hz), 173.4 (d, J = 7.11 Hz). $^{31}P\{^{1}H\}$ NMR ($CDCl_3$, δ ppm): 52.3 (s).

1c: Synthesis of this compound was reported by Lindner et al. with 70% yield [8]. We followed a slightly modified procedure (in an analogous manner to our synthesis of **2c**) from 2.00 g (21.0 mmol) 2-hydroxypyridine, 4.65 g (21.0 mmol) triethylamine and 1.89 g (10.5 mmol) dichlorophenylphosphine. The white crystalline product was obtained in 92% yield (2.86 g, 9.64 mmol). Crystals suitable for single-crystal X-ray diffraction were obtained by crystallization from hot *n*-hexane.

Anal. Calc. for $C_{16}H_{13}N_2O_2P$ (MW: 263.25), requires: C, 64.87; H, 4.42; N, 9.46. Found: C, 64.14; H, 4.69; N, 9.30%. ^{1}H NMR ($CDCl_3$, δ ppm): 6.90–7.00 (m, H^3, H^5, **Lc**, 4H), 7.48 (m, *para*-Ph, *meta*-Ph, 3H), 7.63 (m, H^4, **Lc**, 2H), 7.97 (m, *ortho*-Ph, 2H), 8.14 (m, H^6, **Lc**, 2H). $^{13}C\{^{1}H\}$ NMR ($CDCl_3$, δ ppm): 112.6 (s, J = 1.48 Hz, C^3, **Lc**), 118.6 (s, C^5, **Lc**), 128.4 (d, J = 7.27 Hz, *meta*-Ph), 130.4 (d, J = 26.11 Hz, *ortho*-Ph), 131.0 (s, *para*-Ph), 139.2 (s, C^4, **Lc**), 140.5 (d, J = 18.23 Hz, *ipso*-Ph), 147.4 (s, C^6, **Lc**), 161.8 (d, J = 6.67 Hz, C^2, **Lc**). $^{31}P\{^{1}H\}$ NMR ($CDCl_3$, δ ppm): 148.0 (s).

2a: This compound was synthesized in an analogous manner to **1a** from 900 mg (6.66 mmol) *N*-methylbenzamide, 2.7 mL (6.75 mmol) of a 2.5 M *n*-BuLi solution in hexanes and 305 mg (2.22 mmol) PCl_3. The product was recrystallized from THF (7 mL). The colorless crystalline product was obtained in 23% yield (226 mg, 0.29 mmol).

Anal. Calc. for $C_{24}H_{24}N_3O_3P$ (MW: 433.44), requires: C, 66.50; H, 5.58; N, 9.69. Found: C, 66.38; H, 5.72; N, 9.61%. ^{1}H NMR ($CDCl_3$, δ ppm): 3.18 (d, J = 1.15 Hz, –CH_3, 9H), 7.00 (br. m, aryl, 6H), 7.26 (m, aryl, 6H), 7.39 (m, aryl, 3H). $^{13}C\{^{1}H\}$ NMR ($CDCl_3$, δ ppm): 31.9 (s), 127.2 (d, J = 6.5 Hz), 128.3 (s), 130.5 (s), 135.4 (d, J = 3.2 Hz), 174.6 (d, J = 33.4 Hz). $^{31}P\{^{1}H\}$ NMR ($CDCl_3$, δ ppm): 93.9 (br. s).

2b: This compound was synthesized in an analogous manner to **1b** from 800 mg (6.01 mmol) phthalimidine, 670 mg (6.62 mmol) triethylamine and 275 mg (2.00 mmol) PCl_3. The product was recrystallized from THF (20 mL). The white crystalline product was obtained in 43% yield (431 mg, 0.86 mmol).

Anal. Calc. for $C_{24}H_{18}N_3O_3P$·THF (MW: 499.50), requires: C, 67.33; H, 5.25; N, 8.41. Found: C, 66.55; H, 5.25; N, 8.31%. ^{1}H NMR ($CDCl_3$, δ ppm): 4.89 (s, –CH_2–, 6H), 7.47 (m, aryl, 6H), 7.60 (dd, J = 7.59 Hz, J = 7.13 Hz, aryl, 3H), 7.83 (d, J = 7.59 Hz, aryl, 3H). $^{13}C\{^{1}H\}$ NMR ($CDCl_3$, δ ppm): 51.2 (d, J = 8.6 Hz), 123.2 (s), 124.3 (s), 128.3 (s), 131.3 (s), 132.9 (s), 144.5 (d, J = 5.5 Hz), 172.8 (d, J = 11.5 Hz). $^{31}P\{^{1}H\}$ NMR ($CDCl_3$, δ ppm): 67.4 (s).

2c: Synthesis of this compound was reported by Weigand et al. with 30% yield [17]. In an attempt at improving the yield we used a modified procedure: To a solution of 2-hydroxypyridine (500 mg, 5.26 mmol) and triethylamine (532 mg, 5.26 mmol) in THF (10 mL) at room temperature PCl_3 (241 mg, 1.75 mmol) was added with stirring. The white suspension was stirred at ambient temperature for 3 h, then filtered and the white solid was washed with THF (3 mL). The combined filtrate and washings were evaporated to dryness (condensation of volatiles into a cold trap under reduced pressure) and the residue was recrystallized from THF (1 mL). After three weeks storage at −24 °C colorless crystals were obtained. The supernatant was removed by decantation, the white solid was washed with *n*-pentane (3 mL) and dried *in vacuo*. Yield: 286 mg (0.91 mmol, 52%). The compound is highly hygroscopic.

Anal. Calc. for $C_{15}H_{12}N_3O_3P$·1.3H_2O (MW: 336.67), requires: C, 53.51; H, 4.37; N, 12.48. Found: C, 53.63; H, 4.54; N, 12.43%. NMR data (^{1}H, ^{13}C, ^{31}P) correspond to the data reported in [17].

*2.5. Syntheses of Ru-complexes **3a**, **3b**, **3c**, **4b**, **4c**, **5a**, **6**, **7b** and **7c***

3a: **1a** (91 mg, 226 μmol) and [$RuCl_2(PPh_3)_3$] (219 mg, 228 μmol) were dissolved in $CHCl_3$ (3 mL). The deep red solution was stirred at room temperature for 10 min. After vapor diffusion of Et_2O (for one week) and formation of crystalline material during that time, the supernatant was removed by decantation, the crude yellow solid was dispersed in 10 mL $CHCl_3$, filtered, washed with $CHCl_3$ (1 mL) and dried *in vacuo*. Yield: 44 mg (46 μmol, 20%). Yellow crystals, suitable for single-crystal X-ray diffraction, were obtained by vapor diffusion of Et_2O into a CH_2Cl_2 solution within one week. Although the crystal structure reveals the formation of a dichloromethane solvate **3a**·$3CH_2Cl_2$, the elemental composition upon drying corresponds to lower solvent content.

Anal. Calc. for $C_{40}H_{36}Cl_2N_2O_2P_2Ru{\cdot}1.2CHCl_3$ (MW: 953.90), requires: C, 51.88; H, 3.93; N, 2.94. Found: C, 51.87; H, 4.12; N, 2.81%. ^{1}H NMR (CD_2Cl_2, δ ppm): 3.28 (d, J = 4.64 Hz, –CH_3, 3H), 3.30 (d, J = 4.45 Hz, –CH_3, 3H), 6.95–7.01 (m, aryl, 6H), 7.02–7.09 (m, aryl, 5H), 7.32–7.38 (m, aryl, 2H), 7.43–7.50 (m, aryl, 3H), 7.51–7.66 (br. m, aryl, 14H). ^{13}C{^{1}H} NMR (CD_2Cl_2, δ ppm): 38.2 (d, J = 3.98 Hz, -CH_3), 38.9 (d, J = 4.55 Hz, -CH_3), 126.3 (d, J = 62.51 Hz, *ipso*-PPh), 127.6 (d, J = 9.85 Hz, *meta*-PPh_3), 127.9 (s), 128.4 (s), 128.9 (s), 129.1 (s), 129.2 (d, J = 2.08 Hz, *para*-PPh_3), 130.4 (d, J = 11.36 Hz), 130.7 (d, J = 5.68 Hz), 131.6 (d, J = 12.18 Hz), 131.8 (s), 132.4 (s), 133.2 (s), 133.4 (m), 134.1 (d, J = 9.63 Hz, *ortho*-PPh_3), 134.4 (d, J = 47.73 Hz, *ipso*-PPh_3), 184.7 (m), 184.8 (m). ^{31}P{^{1}H} NMR (CD_2Cl_2, δ ppm): 166.6 (d, J = 38 Hz, PhP(**La**)$_2$, 1P), 54.1 (d, J = 38 Hz, PPh_3, 1P).

3b: **1b** (210 mg, 564 μmol) and [$RuCl_2(PPh_3)_3$] (540 mg, 563 μmol) were dissolved in $CHCl_3$ (30 mL). The red solution was stirred for 2 h at room temperature to form an orange suspension, which was then filtered, the orange solid was washed with $CHCl_3$ (2 mL) and dried *in vacuo*. Yield: 310 mg (326 μmol, 58%). Orange crystals, suitable for single-crystal X-ray diffraction, were obtained by vapor diffusion of Et_2O into a $CHCl_3$ solution. Although the crystal structure reveals the formation of a chloroform solvate **3b**·$1.95CHCl_3$, the elemental composition upon drying corresponds to lower solvent content.

Anal. Calc. for $C_{40}H_{32}Cl_2N_2O_2P_2Ru{\cdot}1.2CHCl_3$ (MW: 949.87), requires: C, 52.10; H, 3.52; N, 2.95. Found: C, 52.23; H, 3.37; N, 3.09%. ^{1}H NMR (CD_2Cl_2, δ ppm): 4.51 (d, J = 17.12 Hz, –CH_2–, 2H), 4.90 (d, J = 17.12 Hz, –CH_2–, 1H), 4.99 (d, J = 17.12 Hz, –CH_2–, 1H), 6.98 (m, aryl, 6H), 7.05 (m, aryl, 3H), 7.28–7.39 (br. m, aryl, $CHCl_3$, 3.2H), 7.44 (m, aryl, 4H), 7.50–7.73 (br. m, aryl, 12H), 8.16 (d, J = 7.69 Hz, aryl, 1H). ^{31}P{^{1}H} NMR (CD_2Cl_2, δ ppm): 127.2 (d, J = 43.5 Hz, PhP(**Lb**)$_2$, 1P), 57.0 (d, J = 43.5 Hz, PPh_3, 1P).

3c: **1c** (154 mg, 519 μmol) and [$RuCl_2(PPh_3)_3$] (498 mg, 519 μmol) were dissolved in $CHCl_3$ (3 mL). The orange solution was stirred for 10 min at room temperature and then filtered through Celite. After four days, orange crystals, suitable for single-crystal X-ray diffraction, were obtained by vapor diffusion of Et_2O into the filtrate. The supernatant was decanted, the solid was washed with Et_2O (2 mL) and dried *in vacuo*. Yield: 312 mg (343 μmol, 66%).

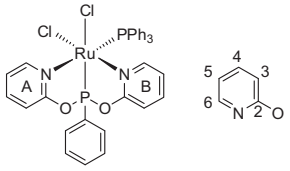

Anal. Calc. for $C_{34}H_{28}Cl_2N_2O_2P_2Ru{\cdot}1.5CHCl_3$ (MW: 909.59), requires: C, 46.88; H, 3.27; N, 3.08. Found: C, 46.96; H, 3.29; N, 3.16%. ^{1}H NMR ($CDCl_3$, δ ppm): 6.28 (ddd, J = 1.38 Hz, J = 6.13 Hz, J = 7.46 Hz, H^{5B}, 1H), 6.87 (d, J = 8.10 Hz, H^{3B}, 1H), 6.90–6.98 (m, *meta*-PPh_3, 6H), 7.00–7.09 (m, *para*-PPh_3, H^{3A}, 4H), 7.11 (m, H^{5A}, 1H), 7.27–7.34 (m, *meta*-PPh, H^{4B}, 3H), 7.52 (t, J = 7.61 Hz, *para*-PPh, 1H), 7.59–7.69 (m, *ortho*-PPh_3, H^{4A}, 7H), 7.75 (m, *ortho*-PPh, 2H), 8.80 (dd, J = 1.69 Hz, J = 6.13 Hz, H^{6B}, 1H), 9.78 (br. m, H^{6A}, 1H). ^{13}C{^{1}H} NMR ($CDCl_3$, δ ppm): 109.8 (d, J = 7.13 Hz, C^{3B}), 110.5 (d, J = 6.29 Hz, C^{3A}), 118.9 (s, C^{5B}), 120.0 (d, J = 2.74 Hz, C^{5A}), 127.3 (d, J = 9.65 Hz, *meta*-PPh_3), 128.7 (d, J = 12.37 Hz, *meta*-PPh), 128.8 (d, J = 2.15 Hz, *para*-PPh_3), 130.6 (d, J = 78.9 Hz, *ipso*-PPh), 130.8 (d, J = 12.84 Hz, *ortho*-PPh), 132.3 (d, J = 1.41 Hz, *para*-PPh), 133.5 (d, J = 9.41 Hz, *ortho*-PPh_3), 133.6 (d, J = 45.0 Hz, *ipso*-PPh_3), 137.8 (s, C^{4B}), 140.1 (s, C^{4A}), 149.9 (s, C^{6A}), 152.6 (s, C^{6B}), 161.7 (m, C^{2A}), 162.4 (d, J = 2.27 Hz, C^{2B}). ^{31}P{^{1}H} NMR ($CDCl_3$, δ ppm): 210.7 (d, J = 37.2 Hz, PhP(**Lc**)$_2$, 1P), 41.0 (d, J = 37.2 Hz, PPh_3, 1P).

4b: This compound was synthesized in an analogous manner to **3c** from 65 mg (130 μmol) **2b** and 125 mg (130 μmol) [$RuCl_2(PPh_3)_3$] in 10 mL CH_2Cl_2. The orange crystalline product was obtained in 76% yield (92 mg, 99 μmol). Although the crystal structure reveals the formation of a dichloromethane solvate **4b**·$2CH_2Cl_2$, the elemental composition upon drying corresponds to lower solvent content.

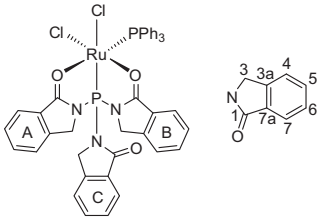

Anal. Calc. for $C_{42}H_{33}Cl_2N_3O_3P_2Ru{\cdot}CH_2Cl_2$ (MW: 946.58), requires: C, 54.56; H, 3.73; N, 4.44. Found: C, 54.34; H, 3.56; N, 4.47%. ^{1}H NMR ($CDCl_3$, δ ppm): 4.45 (d, J = 17.20 Hz, H^{3C}, 1H), 4.84 (m, $H^{3A/C}$, 2H), 4.97 (d, J = 16.62 Hz, H^{3A}, 1H), 5.10 (d, J = 17.37 Hz, H^{3B}, 1H), 5.40 (d, J = 17.37 Hz, H^{3B}, 1H), 6.91–7.01 (m, *meta*-PPh_3, *para*-PPh_3, 9H), 7.19 (d, J = 7.75 Hz, H^{7B}, 1H), 7.27 (m, H^{6B}, 1H), 7.32 (d, J = 7.60 Hz, H^{4C}, 1H), 7.36 (d, J = 7.75 Hz, H^{4B}, 1H), 7.42 (d, J = 7.55 Hz, H^{4A}, 1H), 7.50 (m, H^{6A}, H^{5B}, H^{6C}, 3H), 7.58 (dd, J = 7.55 Hz, J = 8.16 Hz, H^{5A}, 1H), 7.66 (m, H^{5C}, H^{7C}, 2H), 7.90 (m, *ortho*-PPh_3, 6H), 8.13 (d, J = 7.76 Hz, H^{7A}, 1H). ^{13}C{^{1}H} NMR ($CDCl_3$, δ ppm): 50.3 (m, C^{3A}), 51.4 (d, J = 14.5 Hz, C^{3C}), 53.0 (m, C^{3B}), 123.2 (s, C^{4C}), 123.3 (s, C^{4B}), 123.5 (s, C^{4A}), 124.7 (s, C^{7C}), 125.2 (s, C^{7B}), 126.1 (m, C^{7aB}), 126.3 (s, C^{7A}), 127.5 (d, J = 10.1 Hz, *meta*-PPh_3), 128.1 (s, C^{6B}), 128.4 (s, C^{6C}), 129.2 (s, C^{6A}, *para*-PPh_3), 130.0 (m, C^{7aC}), 132.1 (m, C^{7aA}), 133.5–134.4 (br. m, C^{5A}, C^{5B}, C^{5C}, *ipso*-PPh_3, *ortho*-PPh_3), 144.4 (m, C^{3aC}), 146.0 (s, C^{3aA}), 146.8 (s, C^{3aB}), 171.1 (s, C^{1C}), 180.8 (m, C^{1A}), 183.1 (d, J = 19.3 Hz, C^{1B}). ^{31}P{^{1}H} NMR ($CDCl_3$, δ ppm): 123.6 (d, J = 48.9 Hz, P(**Lb**)$_3$, 1P), 52.6 (d, J = 48.9 Hz, PPh_3, 1P).

4c: This compound was synthesized in an analogous manner to **3c** from 156 mg (498 μmol) **2c** and 478 mg (498 μmol) [$RuCl_2(PPh_3)_3$] in 10 mL $CHCl_3$. The yellow fine crystalline product was obtained in 69% yield (285 mg, 345 μmol). The presence of the solvents used to interpret the elemental composition was confirmed by ^{1}H NMR spectroscopy.

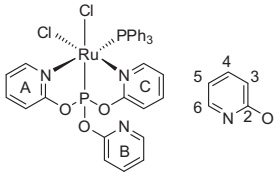

Anal. Calc. for $C_{33}H_{27}Cl_2N_3O_3P_2Ru{\cdot}0.4CHCl_3{\cdot}0.4Et_2O$ (MW: 824.91), requires: C, 50.96; H, 3.84; N, 5.09. Found: C, 50.98; H, 3.81; N, 5.10%. ^{1}H NMR ($CDCl_3$, δ ppm): 6.33 (dd, J = 6.15 Hz, J = 7.63 Hz, H^{5C}, 1H), 6.74 (d, J = 7.99 Hz, H^{3C}, 1H), 7.02 (m, H^{3A}, *meta*-PPh_3, 7H), 7.13 (m, H^{5A}, *para*-PPh_3, 4H), 7.19 (dd, J = 4.87 Hz, J = 6.83 Hz, H^{5B}, 1H), 7.30 (m, H^{4C}, 1H), 7.31 (m, H^{3B}, 1H), 7.69 (dd, J = 7.70 Hz, J = 8.43 Hz, H^{4A}, 1H), 7.76 (m, H^{4B}, 1H), 7.80 (dd, J = 8.84 Hz, J = 10.89 Hz, *ortho*-PPh_3, 6H), 8.29 (dd, J = 4.87 Hz, H^{6B}, 1H), 8.89 (dd, J = 6.15 Hz, H^{6C}, 1H), 9.66 (m, H^{6A}, 1H). $^{13}C\{^1H\}$ NMR ($CDCl_3$, δ ppm): 109.8 (d, J = 8.34 Hz, C^{3C}), 110.5 (d, J = 7.30 Hz, C^{3A}), 114.0 (d, J = 4.35 Hz, C^{3B}), 118.8 (s, C^{5C}), 120.0 (d, J = 2.0 Hz, C^{5A}), 121.1 (s, C^{5B}), 127.6 (d, J = 9.56 Hz, *meta*-PPh_3), 129.1 (d, J = 1.67 Hz, *para*-PPh_3), 133.8 (d, J = 9.60 Hz, *ortho*-PPh_3), 134.0 (d, J = 43 Hz, *ipso*-PPh_3), 138.3 (s, C^{4C}), 140.2 (s, C^{4B}), 140.6 (s, C^{4A}), 147.9 (s, C^{6B}), 150.0 (s, C^{6A}), 152.4 (s, C^{6C}), 157.4 (d, J = 6.75 Hz, C^{2B}), 160.7 (d, J = 6.41 Hz, C^{2A}), 160.9 (d, J = 6.58 Hz, C^{2C}). $^{31}P\{^1H\}$ NMR ($CDCl_3$, δ ppm): 166.4 (d, J = 51.1 Hz, P(**Lc**)$_3$, 1P), 41.7 (d, J = 51.1 Hz, PPh_3, 1P).

5a: **2a** (500 mg, 1.15 mmol) and $[RuCl_2(PPh_3)_3]$ (1.11 g, 1.15 mmol) were dissolved in THF (5 mL) and heated under reflux for 3 h. During that time yellow solid precipitated. After cooling to room temperature the suspension was filtered and the yellow solid was washed with THF (2 × 2 mL) and dried *in vacuo*. Yield: 53% (646 mg, 616 µmol). Crystals of **5a**, suitable for single-crystal X-ray diffraction, were obtained by recrystallization in THF. Although the crystal structure reveals the formation of a THF solvate **5a**·3THF, the elemental composition upon drying corresponds to lower solvent content.

Anal. Calc. for $C_{52}H_{46}ClN_2O_3P_3Ru{\cdot}THF$ (MW: 1048.48), requires: C, 64.15; H, 5.19; N, 2.67. Found: C, 63.90; H, 5.09; N, 2.35%. ^{1}H NMR ($CDCl_3$, δ ppm): 2.90 (d, J = 3.80 Hz, –CH_3, 6H), 6.93 (m, *ortho*-Ph, 4H), 7.08 (dd, J = 7.60 Hz, J = 8.19 Hz, *meta*-PPh_3, 12H), 7.20 (m, *meta*-Ph, *para*-PPh_3, 10H), 7.33 (tm, J = 7.51 Hz, *para*-Ph, 2H), 7.54 (m, *ortho*-PPh_3, 12H). $^{13}C\{^1H\}$ NMR ($CDCl_3$, δ ppm): 32.6 (s, –CH_3), 127.2 (dd, J = 5.77 Hz, J = 4.59 Hz, *meta*-PPh_3), 127.8 (s, *meta*-Ph), 128.3 (s, *ortho*-Ph), 129.0 (s, *para*-PPh_3), 130.9 (s, *para*-Ph), 132.2 (s, *ipso*-Ph), 134.5 (m, *ipso*-PPh_3), 135.1 (dd, J = 5.83 Hz, J = 4.71 Hz, *ortho*-PPh_3), 177.8 (d, J = 11.81 Hz, NCO). $^{31}P\{^1H\}$ NMR ($CDCl_3$, δ ppm): 142.8 (t, J = 44.3 Hz, OP(**La**)$_2$, 1P), 47.2 (d, J = 44.3 Hz, PPh_3, 2P).

The combined filtrated and washings were treated with $TlPF_6$ (403 mg, 1.15 mmol) and stirred at room temperature for 3 h. The suspension was filtered through Celite and the filtrate was evaporated to dryness under reduced pressure. Attempts to isolate **6** in pure state from this residue, i.e., by recrystallization from $CHCl_3$ or THF solutions upon vapor diffusion of Et_2O, failed. However, a small amount of crystals of **6**, suitable for single-crystal X-ray diffraction, were obtained by vapor diffusion of Et_2O into a $CHCl_3$ solution of the crude reaction mixture of $[RuCl_2(PPh_3)_3]$, **2a** and $TlPF_6$.

$^{31}P\{^1H\}$ NMR ($CDCl_3$, δ ppm): 15.1 (s, $Ph_3P(Ph)C=NMe^+$, 1P), −144.5 (sept., J = 713 Hz, PF_6^-, 1P).

7b: **2b** (69 mg, 138 µmol) and $[RuCl_2(PPh_3)_3]$ (132 mg, 138 µmol) were dissolved in $CHCl_3$ (10 mL). The orange solution was stirred for 15 min at room temperature, whereupon solid $TlPF_6$ (98 mg, 281 µmol) was added and the yellow suspension was stirred at room temperature for 1 h and then filtered through Celite. After four days, yellow crystals, suitable for single-crystal X-ray diffraction, were obtained by vapor diffusion of Et_2O into the filtrate. The supernatant was decanted, the solid was washed with Et_2O (3 mL) and dried *in vacuo*. Yield: 107 mg (78 µmol, 57%). Although the crystal structure reveals the formation of a solvate **7b**·$CHCl_3{\cdot}2Et_2O$, the elemental composition upon drying corresponds to lower diethyl ether content.

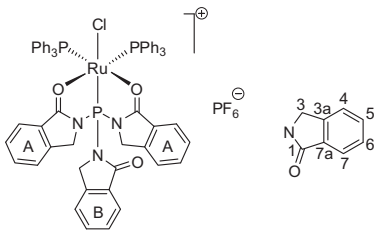

Anal. Calc. for $C_{60}H_{48}ClF_6N_3O_3P_4Ru{\cdot}CHCl_3{\cdot}0.25Et_2O$ (MW: 1371.36), requires: C, 54.30; H, 3.79; N, 3.06. Found: C, 54.60; H, 3.81; N, 3.22%. ^{1}H NMR ($CDCl_3$, δ ppm): 3.46 (m, H^{3B}, 2H), 4.96 (d, J = 17.94 Hz, H^{3A}, 2H), 5.09 (d, J = 17.94 Hz, H^{3A}, 2H), 6.99 (dd, J = 7.42 Hz, J = 7.75 Hz, *meta*-PPh_3, 12H), 7.13 (t, J = 7.42 Hz, *para*-PPh_3, 6H), 7.29 (d, J = 7.70 Hz, H^{4B}, 1H), 7.36 (dd, J = 7.65 Hz, J = 7.45 Hz, H^{6A}, 2H), 7.45 (m, H^{7B}, 1H), 7.48 (m, H^{6B}, H^{7A}, 3H), 7.54 (d, J = 7.70 Hz, H^{4A}, 2H), 7.59 (m, H^{5A}, *ortho*-PPh_3, 14H), 7.72 (m, H^{5B}, 1H). $^{13}C\{^1H\}$ NMR ($CDCl_3$, δ ppm): 49.7 (d, J = 7.0 Hz, C^{3B}), 52.5 (d, J = 6.1 Hz, C^{3A}), 123.4 (s, C^{4B}), 124.5 (s, C^{4A}), 124.8 (s, C^{7B}), 125.2 (s, C^{7A}), 125.8 (d, J = 4.0 Hz, C^{7aA}), 127.8 (m, *meta*-PPh_3), 128.5 (s, C^{6A}), 128.7 (s, C^{6B}), 129.2 (d, J = 5.3 Hz, C^{7aB}), 130.2 (s, *para*-PPh_3), 133.6 (br. m, *ipso*-PPh_3), 134.7 (m, C^{5B}, *ortho*-PPh_3), 135.0 (m, C^{5A}), 143.5 (d, J = 8.5 Hz, C^{3aB}), 147.7 (s, C^{3aA}), 171.0 (s, C^{1B}), 182.5 (d, J = 18.0 Hz, C^{1A}). $^{31}P\{^1H\}$ NMR ($CDCl_3$, δ ppm): 128.0 (t, J = 39.0 Hz, P(**Lb**)$_3$, 1P), 40.4 (d, J = 39.0 Hz, PPh_3, 2P), −144.3 (sept., J = 713 Hz, PF_6^-, 1P).

7c: This compound was synthesized in an analogous manner to **7b** from 110 mg (351 µmol) **2c**, 337 mg (351 µmol) $[RuCl_2(PPh_3)_3]$ and 300 mg (859 µmol) $TlPF_6$ in 10 mL $CHCl_3$. The yellow crystalline product was obtained in 75% yield (324 mg, 263 µmol). Although the crystal structure reveals the formation of a chloroform solvate **7c**·$CHCl_3$, the elemental composition of the bulk material indicates mixed solvates of chloroform and diethyl ether.

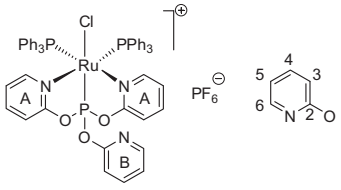

Anal. Calc. for $C_{51}H_{42}ClF_6N_3O_3P_4Ru{\cdot}0.8CHCl_3{\cdot}0.2Et_2O$ (MW: 1229.63), requires: C, 51.38; H, 3.67; N, 3.42. Found: C, 51.52; H, 3.59; N, 3.46%. ^{1}H NMR (CD_2Cl_2, δ ppm): 6.77 (m, H^{3A}, H^{5A}, 4H), 7.03 (d, J = 8.12 Hz, H^{3B}, 1H), 7.09 (dd, J = 7.50 Hz, J = 8.02 Hz, *meta*-PPh_3, 12H), 7.30 (t, J = 7.50 Hz, *para*-PPh_3, $CHCl_3$, 6.8H), 7.39 (m, *ortho*-PPh_3, 12H), 7.48 (ddd, J = 7.34 Hz, J = 4.88 Hz, J = 0.75 Hz, H^{5B}, 1H), 7.53 (ddd, J = 7.83 Hz, J = 7.76 Hz, J = 1.43 Hz, H^{4A}, 2H), 8.01 (ddd, J = 8.12 Hz, J = 7.34 Hz, J = 2.04 Hz, H^{4B}, 1H), 8.55 (ddd, J = 4.88 Hz, J = 2.04 Hz, J = 0.60 Hz, H^{6B}, 1H), 8.92 (dm, J = 6.03 Hz, H^{6A}, 2H). $^{13}C\{^1H\}$ NMR (CD_2Cl_2, δ ppm): 112.2 (d, J = 7.84 Hz, C^{3A}), 115.0 (d, J = 3.22 Hz, C^{3B}), 121.3 (s, C^{5A}), 123.7 (s, C^{5B}), 128.3 (dd, J = 5.66 Hz, J = 4.80 Hz, *meta*-PPh_3), 130.7 (s, *para*-PPh_3), 132.6 (m, *ipso*-PPh_3), 135.0 (dd, J = 5.60 Hz, J = 4.75 Hz, *ortho*-PPh_3), 141.6 (s, C^{4B}), 142.2 (s, C^{4A}), 148.9 (s, C^{6A}), 149.1 (s, C^{6B}), 157.3 (s, J = 22.53 Hz, C^{2B}), 160.4 (s, J = 5.37 Hz, C^{2A}). $^{31}P\{^1H\}$ NMR (CD_2Cl_2, δ ppm): 162.6 (t, J = 48 Hz, P(**Lc**)$_3$, 1P), 36.4 (d, J = 48 Hz, PPh_3, 2P), −144.5 (sept., J = 713 Hz, PF_6^-, 1P).

3. Results and discussion

3.1. Chelating ligands

The reaction of $PhPCl_2$ or PCl_3 with the lithium salt of *N*-methylbenzamide (**HLa**) or, in presence of triethylamine, with phthalim-

idine (**HLb**) or 2-hydroxypyridine (**HLc**) gave the *N*-substituted derivatives **1a**, **2a**, **1b** and **2b** and the expected *O*-substituted derivatives **1c** and **2c** in an analogous manner to their diphenylphosphino-functionalized homologs (Scheme 2) [1]. As reported for the PPh_2 derivatives [1], in the $^{13}C\{^1H\}$ NMR spectrum we observed the characteristic $^2J_{P,C}$ coupling of the carbon atoms in direct contiguity of the N atoms for **1a**, **2a**, **1b** and **2b**, supporting the N-P bonding situation, and of the carbon atoms in direct contiguity of the O atoms for **1c** and **2c**, supporting the O–P bonding situation. The ^{31}P NMR shifts of the series $Ph_xP(\mathbf{L})_{3-x}$ (x = 2,1,0) for the naphtholactame derivatives with N–P moiety [2] exhibit a downfield shift in the sequence $\delta^{31}P$ ($x = 2 < 1 < 0$) (Table 1). This behavior is also visible (and more pronounced) for the **HLa** and **HLb** derivatives. For the complete series $Ph_xP(\mathbf{L})_{3-x}$ of phosphino-functionalized **HLa** and **HLb**, we determined the molecular structures by single-crystal X-ray diffraction (Figs. 1 and 2). As depicted, the P–N–C–O sequence in **1a** and **2a** are in the zigzag arrangement, whereas in **1b** and **2b** a U-shape is found. For the latter, the P···O separations are in the range between 2.931(1) and 3.240 (1) Å. The phenyl groups at the *N*-methylbenzamidyl fragment in **1a** and **2a** are stepwise forming a calyx around the P atoms from **1a** to **2a**. The P–N bonds between **1a** and **1b** or **2a** and **2b** are equal or longer for **HLa** (Table 2), similar to their diphenylphosphino-functionalized homologs. The N–P–N angles are significantly larger in **1a** and **2a** than in **1b** and **2b**, respectively. The similar structure differences along the series $Ph_xP(\mathbf{L})_{3-x}$ (x = 2,1,0; **L** = *N*-methylbenzamidyl, phthalimidyl) explain the almost constant upfield shift of the ^{31}P NMR signals of $Ph_xP(\mathbf{Lb})_{3-x}$ relative to the corresponding ^{31}P NMR signals of $Ph_xP(\mathbf{La})_{3-x}$, by about 30 ppm ($\Delta(\delta^{31}P)$ = −27.3 [1] (x = 2), −32.1 (x = 1), −26.5 ppm (x = 0)).

In contrast to the series with **La** and **Lb**, along the series $Ph_xP(\mathbf{Lc})_{3-x}$ (x = 2,1,0; **Lc** = 2-pyridyloxy), we found a sagging pattern of the ^{31}P NMR shifts, which has also been observed for the series $Ph_xP(OPh)_{3-x}$ (x = 2,1,0) [22,23]. The molecular structures of $Ph_xP(\mathbf{Lc})_{3-x}$ (x = 2 [1], 1 (Fig. 1), 0 [17]) determined by single-crystal X-ray diffraction underpin the formation of *O*-phosphino derivatives for all **Lc** fragments, driven by the retention of the aromatic character of the pyridine moiety.

3.2. Neutral ruthenium(II) bis-chelates $[RuCl_2(PPh_3)(PR(\mathbf{L}_2))]$ (R = Ph, **L**; **L** = **La**, **Lb**, **Lc**)

The reaction of the 16e⁻ complex $[RuCl_2(PPh_3)_3]$ with **1a**,**b**,**c** and **2b**,**c** leads (in all five cases) to the formation of the corresponding *all-cis* complexes **3a**,**b**,**c** and **4b**,**c**, respectively, by liberation of two equivalents of triphenylphosphine (Scheme 3). In addition to the ^{31}P NMR signals of **3a** (167.9 ppm, d, J = 38.2 Hz; 54.4 ppm, d, J = 38.2 Hz) and PPh_3 (−5.4 ppm), the $^{31}P\{^1H\}$ NMR spectrum of

Table 1
^{31}P NMR shifts of phosphines of the type $Ph_xP(\mathbf{L})_{3-x}$ in $CDCl_3$ (ppm).

x	La	Lb	1,8-Naphtholactam [2]	Lc	OPh
2	57.0 [1]	29.7 [1]	29.7	100.6 [1]	110.4 [22]
1	85.4	53.3	36.6	148.7 [8]	157.9 [22]
0	93.9	67.4	57.9	133.2	128.6 [23]

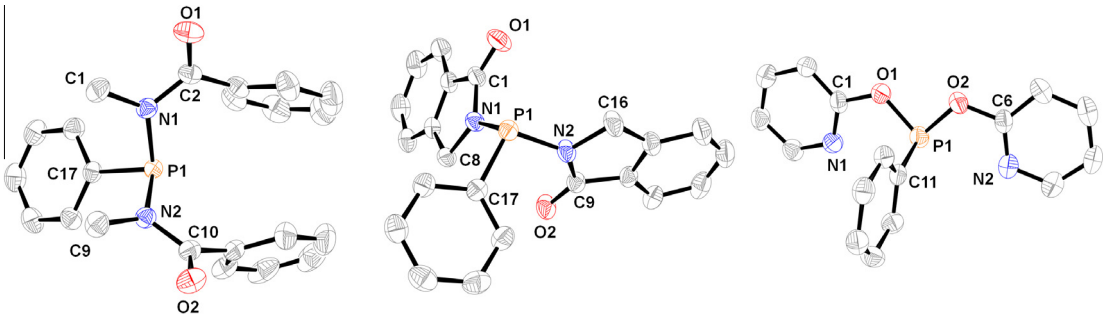

Fig. 1. ORTEP drawing of (from left to right) compound **1a**, **1b** and **1c**. Thermal displacement ellipsoids are displayed at the 50% probability level. H atoms and solvent molecules are omitted for clarity. For **1b** only one of the two crystallographically independent (but conformationally identical) molecules is depicted.

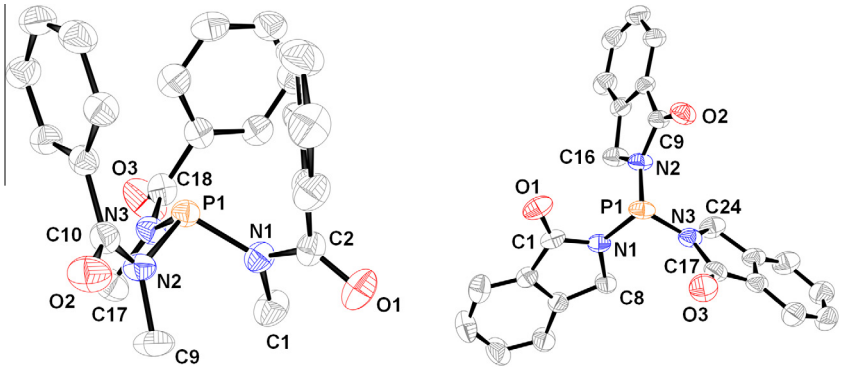

Fig. 2. ORTEP drawing of (from left to right) compounds **2a** and **2b**. Thermal displacement ellipsoids are displayed at the 50% probability level. H atoms and solvent molecules are omitted for clarity.

Please cite this article in press as: R. Gericke, J. Wagler, Polyhedron (2016), http://dx.doi.org/10.1016/j.poly.2016.08.041

Table 2
Selected bond lengths (Å) and angles (°) of **1a**, **1b**, **1c**, **2a**, **2b**.

	1a	1b	1c	2a	2b
P–N/O	1.7287(11) 1.7358(11)	1.7156(12) – 1.7342(12)	1.674(4) 1.675(4)	1.731(4) 1.733(4) 1.740(4)	1.7110(16) 1.7204(14) 1.7251(14)
P–C	1.8220(12)	1.8209(14) 1.8245(14)	1.821(5)		
$C_{carbonyl}$–N	1.3857(17) 1.3872(16)	1.3835(17) – 1.3992(17)	1.318(8) 1.314(8)	1.393(6) 1.385(6) 1.373(6)	1.373(2) 1.388(2) 1.387(2)
$C_{carbonyl}$–O	1.2223(16) 1.2237(16)	1.2189(16) – 1.2250(17)	1.379(6) 1.372(6)	1.218(5) 1.222(6) 1.228(6)	1.217(2) 1.219(2) 1.226(2)
N/O–P–N/O	105.49(5)	103.80(6) 103.92(6)	88.3(2)	100.50(19) 100.88(18) 101.51(19)	98.62(7) 99.30(7) 99.62(7)
C–P–N/O	101.74(6) 100.48(5)	99.68(6) – 103.96(6)	99.1(2) 100.5(2)		
P–N/O–$C_{carbonyl}$	120.77(9) 118.86(9)	118.91(9) – 129.72(9)	116.3(4) 116.7(4)	117.2(3) 116.9(3) 117.2(3)	118.11(11) 118.63(11) 119.76(13)
N–$C_{carbonyl}$–O	120.67(13) 120.90(12)	124.31(13) – 125.89(12)	116.5(5) 116.6(4)	121.9(5) 121.3(4) 121.7(5)	123.63(17) 123.98(18) 124.31(15)

Table 3
Selected bond lengths (Å) and angles (°) of **3a**, **3b** and **3c**.

	3a	3b	3c
Ru1–P1	2.1383(12)	2.1797(6)	2.1328(4)
Ru1–P2	2.2805(12)	2.2965(6)	2.3103(4)
Ru1–N1/O1	2.097(3)	2.1079(15)	2.0906(15)
Ru1–N2/O2	2.146(3)	2.2052(16)	2.1499(14)
Ru1–Cl1	2.3991(11)	2.3894(6)	2.4108(5)
Ru1–Cl2	2.4635(12)	2.4368(6)	2.4602(5)
P1–N1/O1	1.746(4)	1.7388(18)	1.6523(13)
P1–N2/O2	1.753(4)	1.7276(19)	1.6602(13)
P1–C	1.794(5)	1.800(2)	1.7880(17)
$C_{carbonyl}$–N	1.352(6) 1.363(6)	1.369(3) 1.369(3)	1.346(2) 1.337(2)
$C_{carbonyl}$–O	1.263(5) 1.249(6)	1.251(3) 1.246(3)	1.364(2) 1.362(2)
P1–Ru1–N1/O1	81.88(9)	82.39(4)	81.33(4)
P1–Ru1–N2/O2	80.13(9)	81.71(4)	79.62(4)
N1/O1–Ru1–N2/O2	87.42(12)	88.22(6)	86.71(6)
P1–Ru1–P2	99.60(4)	97.43(2)	100.672(16)
P1–Ru1–Cl1	95.60(5)	96.91(2)	94.011(17)
P1–Ru1–Cl2	161.94(5)	164.56(2)	168.256(16)
Cl1–Ru1–Cl2	93.78(4)	88.82(2)	91.584(18)
N1/O1–P1–N2/O2	101.88(19)	101.82(9)	101.78(7)
C–P1–N1/O1	105.48(19)	109.99(10)	99.98(7)
C–P1–N2/O2	101.89(19)	101.20(10)	96.94(7)
C–P1–Ru1	135.56(15)	134.76(8)	140.43(6)
P–N/O–$C_{carbonyl}$	113.8(3) 113.2(3)	113.44(14) 116.10(15)	115.80(11) 116.13(11)
N–C–O	121.8(4) 121.2(4)	124.13(19) 123.5(2)	118.27(15) 118.08(15)

the crude reaction mixture of **1a** and $[RuCl_2(PPh_3)_3]$ in chloroform shows two extra sets of signals (**3a^{I}**: 162.4 ppm, dd, J = 347.6 Hz, J = 35.0 Hz; 47.2 ppm, dd, J = 35.0 Hz, J = 22.2 Hz; 13.4 ppm, dd, J = 347.6 Hz, J = 22.2 Hz; **3a^{III}**: 167.1 ppm, t, J = 29.0 Hz; 38.5 ppm, d, J = 29.0 Hz). Three signals in 1:1:1 ratio with a coupling pattern of an ABX spin system, with characteristic *trans* $^2J_{P,P}$ coupling around 350 Hz and *cis* $^2J_{P,P}$ coupling around 30 Hz, is in support of a structure of a complex **3a^{I}** (Scheme 3), as the signal pattern is similar to its diphenylphosphino analog [1]. With **3a^{I}** as an intermediate, the additional set of two signals in 1:2 ratio with a coupling pattern of an AX_2 spin system can be attributed to a compound with facial arrangement of two chemically equivalent PPh_3 groups and a P atom from ligand **1a**. For the sake of symmetry and chemical equivalence of the two PPh_3 ligands we attribute this set of signals to the ionic compound **3a^{III}**, which should form upon loss of a chloride ion. Attempts to isolate **3a^{III}** by adding PPh_3 to the reaction mixture (in order to hamper the conversion into **3a**) failed.

In addition to the ^{31}P NMR signals of **3b** (127.7 ppm, d, J = 43.5 Hz; 56.8 ppm, d, J = 43.5 Hz) or **4b** (123.6 ppm, d, J = 48.9 Hz; 52.6 ppm, d, J = 48.9 Hz) and PPh_3 (−5.4 ppm), the ^{31}P{^{1}H} NMR spectrum of the crude reaction mixture of **1b** or **2b** and $[RuCl_2(PPh_3)_3]$ in chloroform shows one extra set of signals each (**3b^{I}**: 118.6 ppm, dd, J = 353.4 Hz, J = 38.3 Hz; 48.1 ppm, dd, J = 38.3 Hz, J = 23.7 Hz; 16.0 ppm, dd, J = 353.4 Hz, J = 23.7 Hz; **4b^{I}**: 130.2 ppm, dd, J = 427.9 Hz, J = 46.4 Hz; 48.6 ppm, dd, J = 46.4 Hz, J = 21.4 Hz; 12.2 ppm, dd, J = 427.9 Hz, J = 21.4 Hz, respectively). In each set the signals occur also in 1:1:1 intensity ratio with a coupling pattern of an ABX spin system. In analogy to **3a^{I}** we attribute these signals to compounds **3b^{I}** or **4b^{I}**. Signals of an ionic intermediate (sets of signals which would correspond to those of **3a^{III}**) have not been observed. However, we assume that for all three ligands **1a**,**b** and **2b**, a stepwise replacement of PPh_3 takes place by formation of intermediate **3a^{I}**,**b^{I}** and **4b^{I}** followed by **3a^{III}** and corresponding analogs "**3b^{III}**" and "**4b^{III}**". This stepwise reaction has not been observed for the formation of **3c** or **4c**. This reactivity of the pyridyloxyphosphines is not unexpected: For the related diphenylphosphino derivative Ph_2P-**Lc** we already reported rapid formation of the bis-chelate complex $[RuCl_2(Ph_2P\text{-}\mathbf{Lc})_2]$ without allowing for the detection of the mono-chelate $[RuCl_2(PPh_3)_2(Ph_2P\text{-}\mathbf{Lc})]$ [1]. In the ^{31}P NMR spectra incorporation of ligands **1a**,**b**, **c** and **2b**,**c** in Ru complexes **3a**,**b**,**c** and **4b**,**c**, respectively, causes a significant downfield shift of the ^{31}P resonance by about 30–80 ppm.

For **3a**,**b**,**c** and **4b** the identity of the compound was proven by single-crystal X-ray diffraction structure analyses. In accord with the NMR spectroscopic data in all cases the *all-cis* configuration around the ruthenium atoms was found (Figs. 3 and 4). Selected bond lengths and angles are listed in Tables 3 and 4. The coordination of the Ru atom is distorted octahedral. The Ru1–P2 bond lengths (to PPh_3) are about 2.29 Å, whereas the Ru1–P1 bonds (to the chelating ligand) are much shorter (around 2.14 Å). For **3b** the latter bond is slightly elongated, by about 0.03 Å, in accord

Table 4
Selected bond lengths (Å) and angles (°) of **4b**, **5a**, **7b** and **7c**.

	4b	5a	7b	7c
Ru1–P1	2.138(3)	2.1922(14)	2.2166(6)	2.151(2)
Ru1–P2/P3	2.292(3)	2.3284(14)	2.3634(6)	2.3966(19)
		2.3168(14)	2.3480(6)	2.407(2)
Ru1–N1/O1	2.125(6)	2.167(3)	2.1958(16)	2.207(7)
Ru1–N2/O2	2.175(6)	2.160(4)	2.1261(15)	2.158(6)
Ru1–Cl1	2.401(2)	2.4714(14)	2.4087(5)	2.443(2)
Ru1–Cl2	2.437(2)			
P1–N1/O1	1.715(7)	1.784(5)	1.726(2)	1.625(6)
P1–N2/O2	1.724(7)	1.780(5)	1.726(2)	1.642(6)
P1–N3/O3	1.680(8)	1.483(4)	1.6861(19)	1.563(6)
$C_{carbonyl}$–N	1.364(12)	1.342(8)	1.371(3)	1.342(12)
	1.383(12)	1.348(7)	1.369(3)	1.332(11)
	1.440(11)		1.431(3)	1.302(12)
$C_{carbonyl}$–O	1.234(10)	1.265(7)	1.248(3)	1.381(13)
	1.238(11)	1.264(6)	1.246(3)	1.358(10)
	1.219(10)		1.213(3)	1.423(11)
P1–Ru1–N1/O1	82.25(17)	80.83(10)	79.41(4)	75.82(19)
P1–Ru1–N2/O2	82.49(18)	81.79(10)	81.62(4)	80.14 (19)
N1/O1–Ru1–N2/O2	87.9(2)	82.76(14)	83.73(6)	83.5(2)
P1–Ru1–P2	99.83(9)	98.24(5)	106.75(2)	98.87(8)
P1–Ru1–Cl1	94.73(9)	161.00(5)	159.37(2)	161.03(8)
P1–Ru1–Cl2/P3	162.85(9)	94.01(5)	96.18(2)	98.56(8)
Cl1–Ru1–Cl2	96.09(8)			
P2–Ru–P3		100.68(5)	101.04(2)	100.22(7)
N1/O1–P1–N2/O2	103.0(4)	95.4(2)	101.28(10)	99.5(3)
N3/O3–P1–N1/O1	103.5(4)	106.4(2)	99.84(9)	102.4(3)
N3/O3–P1–N2/O2	99.7(4)	104.8(2)	104.05(10)	101.7(3)
N3/O3–P1–Ru1	139.4(3)	139.18(17)	141.07(8)	134.5(2)
P–N/O–$C_{carbonyl}$	112.7(6)	115.6(4)	113.74(15)	112.8(5)
	114.0(6)	116.3(3)	114.57(15)	118.2(5)
	125.5(6)		128.18(16)	131.5(6)
N–C–O	125.3(8)	121.2(5)	122.9(2)	116.9(7)
	124.5(8)	120.5(5)	123.8(2)	118.1(7)
	123.2(8)		125.1(2)	117.4(8)

with a slightly shorter (by 0.02 Å) *trans* located Ru1–Cl2 bond. The *trans* to PPh_3 located Ru1–N2/O2 bonds are longer by approximately 0.05 Å in comparison to the *trans* to Cl located Ru–N1/O1 bonds. For **3b**, this bond length difference amounts to 0.1 Å. Also, **3b** reveals the smallest Cl1–Ru1–Cl2 angle, which may originate from the set of intramolecular CH···Cl contacts of the *ortho*-H atoms from the phenyl groups, which, in this fashion, is found in **3b** only. Compound **3c** exhibits the largest P1–Ru1–Cl1 angle caused by intramolecular CH···Cl contacts of the H^6 atoms of the 2-pyridyloxy fragments.

3.3. Neutral or cationic ruthenium(II) bis-chelates [RuCl(PPh_3)$_2$(PR(***L***$_2$))](R = O, ***L***; ***L*** = ***La***, ***Lb***, ***Lc***)

Reacting **2a** and [$RuCl_2(PPh_3)_3$] in chloroform in analogous manner to **2b**,**c** did not afford a similar product to **4b**,**c**. Instead compound **5a** was isolated (Scheme 3). In addition to the ^{31}P NMR signals of **5a** (142.8 ppm, t, J = 44.3 Hz; 47.2 ppm, d, J = 44.3 Hz) and PPh_3 (−5.4 ppm), the $^{31}P\{^1H\}$ NMR spectrum of the crude reaction mixture of **2a** and [$RuCl_2(PPh_3)_3$] in chloroform shows two extra sets of signals (**4a^{I}**: 139.5 ppm, dd, J = 416.9 Hz, J = 54.4 Hz; 55.3 ppm, dd, J = 54.4 Hz, J = 13.8 Hz; 10.2 ppm, dd, J = 416.9 Hz, J = 13.8 Hz; **4a^{II}**: 154.2 ppm, dd, J = 48.0 Hz, J = 41.0 Hz; 49.1 ppm, dd, J = 48.0 Hz, J = 32.9 Hz; 41.0 ppm, dd, J = 41.0 Hz, J = 32.9 Hz). The signals of the first ABX spin system occur in 1:1:1 intensity ratio (**4a^{I}**) similar to **3a^{I}**, **3b^{I}** and **4b^{I}**. The signals of **4a^{I}** disappear during the reaction, whereas the signals of a second ABX spin system (1:1:1 ratio) with coupling constants in the typical range of *cis* $^2J_{P,P}$ coupling, were detected as traces in the reaction mixture and were attributed to the isomer **4a^{II}**. For the formation of **5a** we suggest the following route (Scheme 3): At first, one PPh_3 group is replaced by **2a** acting as bidentate ligand forming **4a^{I}**, which isomerizes to **4a^{II}**. After dissociation of one Cl^- ion (similar to **3a^{III}**), **4a^{III}** is formed, where the tripodal ligand is acting as a bis-chelator. The dangling *N*-methylbenzamidyl fragment undergoes an N–P bond cleavage and rearranges to the *O*-phosphino derivative (most likely for steric reasons). Thereafter, the Cl^- ion acts as nucleophile and attacks the carbonyl carbon atom, thus splitting off *N*-methylbenzimidoylchloride (detected by $^{13}C\{^1H\}$ NMR spectroscopy [24]) and simultaneously forming **5a**. Upon adding $TlPF_6$ to the reaction mixture, **6** has been formed instead of *N*-methylbenzimidoylchloride (Scheme 4). In an analogous manner, the reaction mixtures of **2b** or **2c** and [$RuCl_2(PPh_3)_3$] were treated with $TlPF_6$. These reactions did not yield products similar to **5a**. Instead, the reactions terminate at **7b** and **7c** (analogous isomers to **4a^{III}**). In addition to the ^{31}P NMR signals of **7b** (128.0 ppm, t, J = 39.0 Hz; 40.4 ppm, d, J = 39.0 Hz), PPh_3 (−5.4 ppm) and the characteristic $^1J_{P,F}$ coupling of PF_6^- (−144.3 ppm, sept., J = −713.6 Hz), the $^{31}P\{^1H\}$ NMR spectrum of the crude reaction mixture for **2b** and [$RuCl_2(PPh_3)_3$] with $TlPF_6$ in chloroform shows an extra set of signals (**7b^{I}**: 129.9 ppm, dd, J = 428.5 Hz, J = 48.2 Hz; 48.6 ppm, dd, J = 48.2 Hz, J = 22.4 Hz; 12.1 ppm, dd, J = 428.5 Hz, J = 22.4 Hz). The three signals appear in 1:1:1 intensity ratio, as expected. Apparently, compound **4b** is formed first, where the longer Ru–Cl bond *trans* to the chelating ligands P atom (Ru1–Cl2 ≈ 0.04 Å longer than the Ru1–Cl1 bond *trans* to an O atom) is cleaved by $TlPF_6$ to form **7b^{I}**, which isomerizes to **7b**. Formation of an intermediate "**7c^{I}**", which would correspond to **7b^{I}**, could not be detected for the reaction of **2c** and [$RuCl_2(PPh_3)_3$] with $TlPF_6$. As compounds **7b** and **7c** already have a conformation related to compound **5a** (with facial arrangement of the P atoms), a transformation of **7b** into the **5a**-related phthalimidyl-bridged compound was aimed at by adding one equivalent of a chloride ion source (*tetra*-butylammonium chloride) and an additional

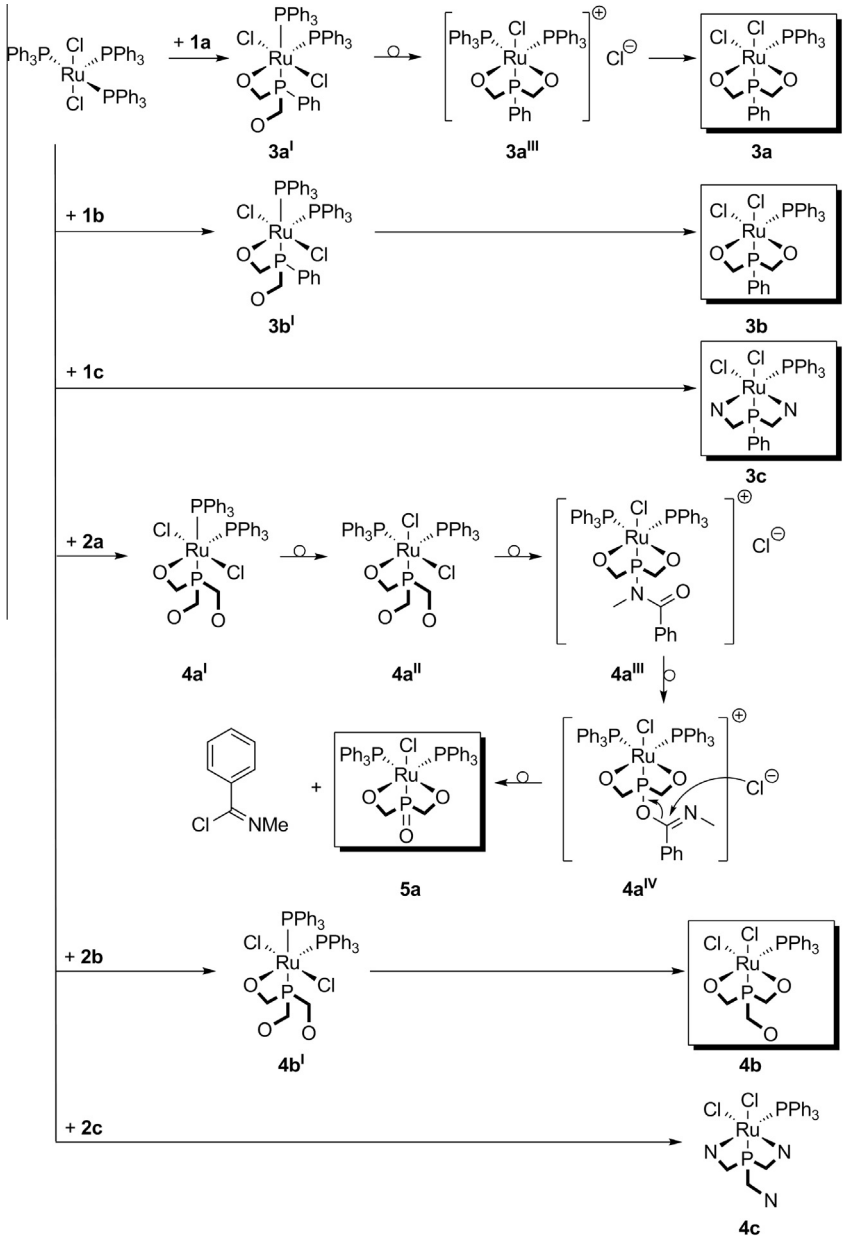

Scheme 3. Synthesis of compounds 3**a**,**b**,**c**, **4b**,**c** and **5a**.

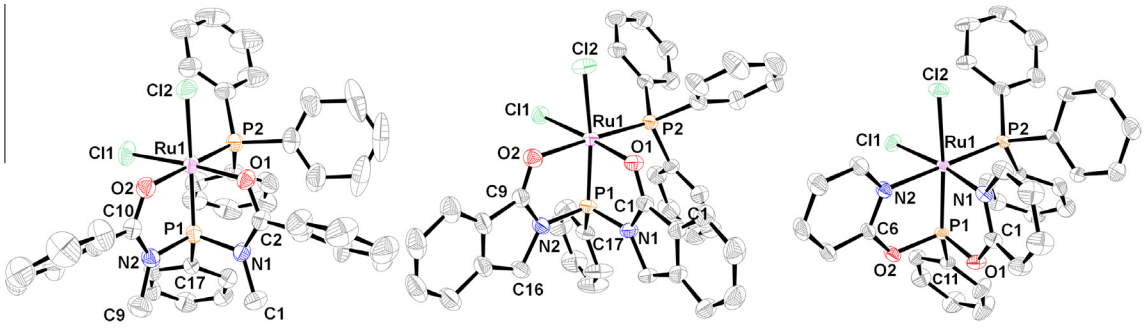

Fig. 3. ORTEP drawing of (from left to right) compound **3a**, **3b** and **3c**. Thermal displacement ellipsoids are displayed at the 50% probability level. H atoms and solvent molecules are omitted for clarity.

equivalent of PPh_3. Instead of nucleophilic attack at the dangling ligand **Lb**, however, slow chloride addition to ruthenium with formation of compound **4b** was observed.

We succeeded in crystallizing (and determining the crystal structures of) all three bis(triphenylphosphine) ruthenium(II) bischelates **5a** and **7b**,**c** (Figs. 4 and 5). All structures show a distorted

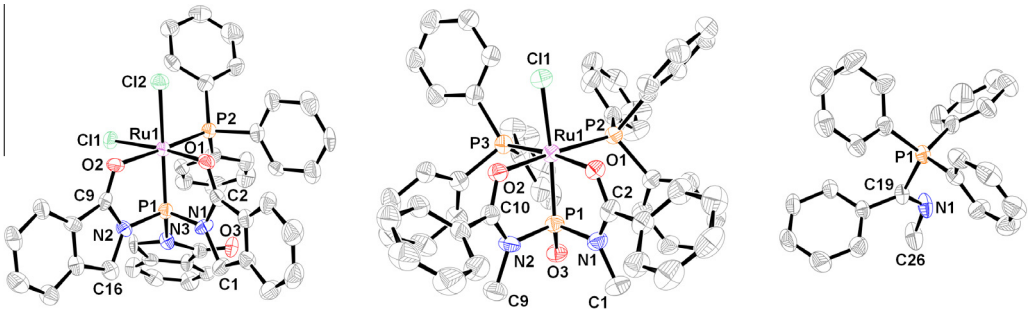

Fig. 4. ORTEP drawing of (from left to right) compound **4b**, **5a** and **6**. Thermal displacement ellipsoids are displayed at the 50% probability level. H atoms, the PF_6^- counterion of **6** and solvent molecules are omitted for clarity.

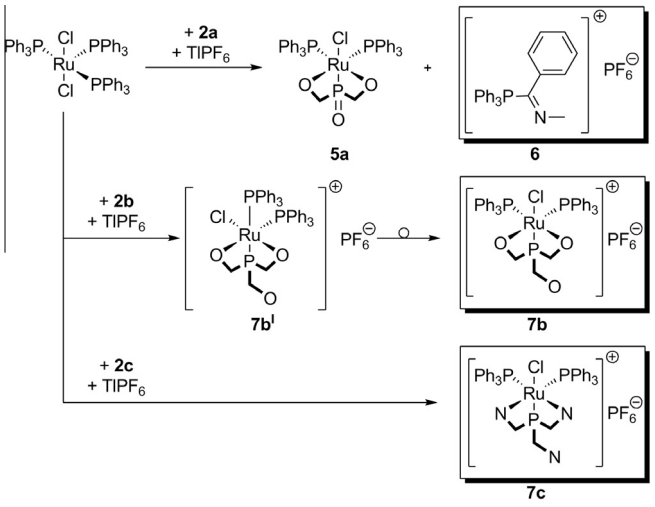

Scheme 4. Synthesis of compounds **5a**, **6**, **7b** and **7c**.

octahedral coordination around the Ru atom with facial arrangement of the phosphorus donors. Although these complexes are structurally related, complex **5a** does not carry a net charge (because of the anionic tridentate O,P,O ligand), whereas **7b** and **7c** are cationic. This difference appears to have some effect on features of the molecular structures. The Ru1–P2 and Ru1–P3 bonds in **7b**,**c** are longer than the corresponding bonds in **5a**, most likely caused by the higher steric demand of the dangling phthalimidyl or 2-pyridyloxy fragment. The cationic net charge of **7b** and **7c**, however, can be assumed to cause the shorter Ru–Cl bonds in these complexes (2.41 and 2.44 Å, respectively), while the negative charge of the tridentate ligand in **5a** may contribute to elongation of the *trans*-disposed Ru–Cl bond (2.47 Å). In contrast, the bond lengths Ru–P1 (**7c** 2.15 Å, **5a** 2.19 Å, **7b** 2.22 Å) do not adhere to systematic differences in ligand charge or steric demand (because of the intermediate position of **5a**) but seem to vary with the PN_xO_{3-x} substitution pattern of P1 (**7c** $x = 3$, **5a** $x = 1$, **7b** $x = 0$) as the Ru–P1 bond is shorter for O-rich (presumably pronounced π-acceptor) phosphorus atoms. The same trend (i.e., dependence on the PN_xO_{3-x} substitution pattern of P1) is reflected by the ^{31}P NMR shifts of P1 (**7c** 162.6 ppm, **5a** 142.8 ppm, **7b** 128.0 ppm) and $^2J_{P,P}$ coupling constants with the *cis*-disposed PPh_3 ligands (**7c** 48 Hz, **5a** 44 Hz, **7b** 39 Hz). The ^{31}P NMR shifts of the PPh_3 ligands, however, reflect the trend of the Ru–PPh_3 bonds (**7c** 36.4 ppm, **7b** 40.4 ppm, **5a** 47.2 ppm), i.e., shift to lower field with decreasing Ru–P bond length.

A closer look at the aromatic range of the ^1H NMR spectra of the pyridyloxyphosphine derivatives **2c**, **3c**, **4c** and **7c** hints at the ^1H resonances of the H^6 atoms as a probe for the pyridyloxy binding mode in these complexes (Fig. 6). In the range 9.4–9.9 ppm a characteristically shaped multiplet is observed for **3c** and **4c**, which is assigned to the **Lc** group *trans*-disposed to a PPh_3 group. The extra coupling is caused by the $^4J_{P,H}$ coupling. In the range 8.7–9.0 this extra coupling is only visible for **7c**, whereas the chemical shift is closer to the corresponding **Lc** groups *trans* located to a chlorine atom as in **3c** and **4c**. Apparently, the coupling pattern (or signal shape arising therefrom) is more characteristic than the chemical shift itself. From 8.1 to 8.6 ppm we observed the typical chemical shift of compound **2c**, which definitely does not coordinate to a Ru atom. For **3c** no signal is detected, as expected, whereas for **4c** and **7c** a signal of the dangling pyridyloxy H^6 is found.

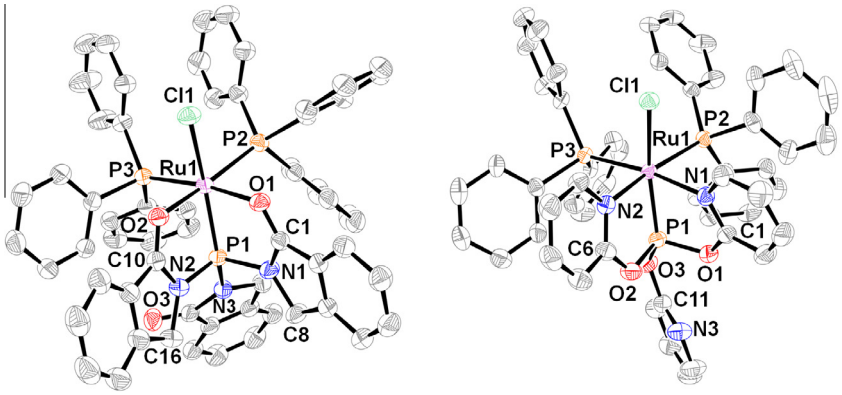

Fig. 5. ORTEP drawing of (from left to right) compound **7b** and **7c**. Thermal displacement ellipsoids are displayed at the 50% probability level. H atoms, PF_6^- counterions and solvent molecules are omitted for clarity.

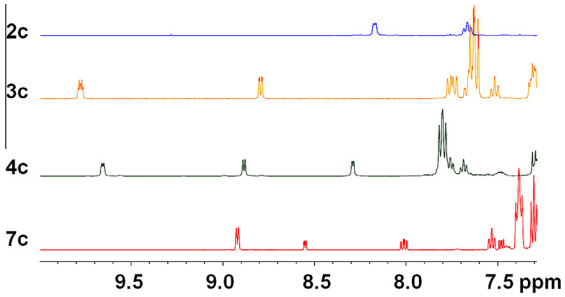

Fig. 6. Selected aromatic range of ^{1}H NMR spectra of **2c**, **3c**, **4c** and **7c**.

4. Conclusions

Four new P,O-chelating ligands (**1a**, **1b**, **2a** and **2b**) and two P,N-chelating ligands (**1c** and **2c**) have been synthesized and their coordination behavior towards ruthenium(II) has been examined. In all cases, regardless of potentially bi- (ligands **1**) or tripodal ligand characteristics (ligands **2**), the final products featured the ambidentate ligand in bipodal O,P,O (ligands **1a**, **1b**, **2a**, **2b**) or N, P,N (ligands **1c**, **2c**) coordination mode. Even treatment with $TlPF_6$ for chloride abstraction did not induce tripodal coordination of ligands **2**. Instead, triphenylphosphine re-filled the vacant coordination site. For the P,O ligands a stepwise PPh_3 replacement has been observed as some intermediates proved to be kinetically inert enough for NMR spectroscopic monitoring. The P,N ligands proved to be more reactive and did not allow for NMR spectroscopic detection of the corresponding kinetically formed intermediates. Interestingly, the *N*-methylbenzamidyl functionalized ligand **2a** undergoes rearrangement and decomposition reactions upon coordination to ruthenium, i.e., formation of a P═O functionalized bipodal ligand, the P═O bond formation presumedly serving as a driving force for the formation of the byproduct PhC(═NMe)Cl. The related ligand **2b** (phthalimidyl functionalized) and ligand **2c** did not undergo such further reactions, even chloride abstraction by addition of $TlPF_6$ only gave rise to cationic complexes with these ligands, the formation of which was reverted upon addition of chloride. Further investigations of this set of ligands **2** in the Ru coordination sphere for exploring the utilization of the third ligand arm, e.g. as tripod functionality, are currently under way.

Acknowledgements

R.G. is grateful to the Studentenwerk Freiberg and the Free State of Saxony for a Ph.D. scholarship (Landesgraduiertenstipendium).

Appendix A. Supplementary data

CCDC 1490791, 1490789, 1490786, 1490788, 1490787, 1490797, 1490794, 1490793, 1490785, 1490795, 1490792, 1490790, 1490796 contains the supplementary crystallographic data for **1a**·0.75THF, **1b**, **1c**, **2a**, **2b**·THF, **3a**·3CH2Cl2, **3b**·1.95CHCl3, **3c**·1.5CHCl3, **4b**·2CH2Cl2, **5a**·3THF, **6**, **7b**·CHCl3·2Et2O, **7c**·CHCl3. These data can be obtained free of charge via http://www.ccdc.cam.ac.uk/conts/retrieving.html, or from the Cambridge Crystallographic Data Centre, 12 Union Road, Cambridge CB2 1EZ, UK; fax: (+44) 1223-336-033; or e-mail: deposit@ccdc.cam.ac.uk. Supplementary data associated with this article can be found, in the online version, at http://dx.doi.org/10.1016/j.poly.2016.08.041.

References

[1] R. Gericke, J. Wagler, Polyhedron (2016), http://dx.doi.org/10.1016/j.poly.2016.06.013.
[2] M. Limmert, I.P. Lorenz, J. Neubauer, A. Schulz, H. Piotrowski, Z. Anorg. Allg. Chem. 629 (2003) 223.
[3] M. Vyšvařil, D. Dastych, J. Taraba, M. Nečas, Inorg. Chim. Acta 362 (2009) 4899.
[4] L.J. Hounjet, M. Bierenstiel, M.J. Ferguson, R. McDonald, M. Cowie, Dalton Trans. (2009) 4213.
[5] P. Braunstein, B.T. Heaton, C. Jacob, L. Manzi, X. Morise, Dalton Trans. (2003) 1396.
[6] A. Kermagoret, F. Tomicki, P. Braunstein, Dalton Trans. (2008) 2945.
[7] C.J. Whiteoak, J.D. Nobbs, E. Kiryushchenkov, S. Pagano, A.J.P. White, G.J.P. Britovsek, Inorg. Chem. 52 (2013) 7000.
[8] E. Lindner, H. Rauleder, W. Hiller, Z. Naturforsch. 38b (1983) 417.
[9] P. Braunstein, M.D. Fryzuk, F. Naud, S.J. Rettig, J. Chem. Soc., Dalton Trans. (1999) 589.
[10] L.D. Field, R.W. Guest, K.Q. Vuong, S.J. Dalgarno, P. Jensen, Inorg. Chem. 48 (2009) 2246.
[11] I. Dahlenburg, S. Kerstan, D. Werner, J. Organomet. Chem. 411 (1991) 437.
[12] L.D. Field, H.L. Li, S.J. Dalgarno, R.D. McIntosh, Inorg. Chem. 52 (2013) 1570.
[13] C. Bianchini, P. Frediani, D. Masi, M. Peruzzini, F. Zanobini, Organometallics 13 (1994) 4616.
[14] M. Visscher, J.C. Huffman, W.E. Streib, Inorg. Chem. 13 (1974) 892.
[15] C. Nave, M.R. Truter, J. Chem. Soc., Dalton Trans. (1978) 2202.
[16] N.A. Bell, S.J. Coles, M.B. Hursthouse, M.E. Light, K.A. Malik, R. Mansor, Polyhedron 19 (2000) 1719.
[17] A.K.C. Echterhoff, S. Yogendra, J. Kösters, R. Fischer, J.J. Weigand, Eur. J. Org. Chem. (2014) 7631.
[18] M.H. Norman, D.J. Minick, G.C. Rigdon, J. Med. Chem. 39 (1996) 149.
[19] S. Hanada, T. Ishida, Y. Motoyama, H. Nagashima, J. Org. Chem. 72 (2007) 7551.
[20] G.M. Sheldrick, Acta Crystallogr., Sect. A 64 (2008) 112.
[21] G.M. Sheldrick, Acta Crystallogr., Sect. C 71 (2015) 3.
[22] S. Lal, J. McNally, A.J.P. White, S. Díez-González, Organometallics 30 (2011) 6225.
[23] I. Thiel, H. Jiao, A. Spannenberg, M. Hapke, Chem. Eur. J. 19 (2013) 2548.
[24] H. Böhme, H.-J. Drechsler, Tetrahedron Lett. 16 (1978) 1429.